Ratio of the Diffusion Coefficient to the Mobility Coefficient for Electrons in He, Ar, N_2, H_2, D_2, CO, and CO_2 at Low Temperatures and Low E/p *

ROGER W. WARREN AND JAMES H. PARKER, JR.
Westinghouse Research Laboratories, Pittsburgh, Pennsylvania
(Received July 23, 1962)

D/μ, the ratio of the diffusion coefficient to the mobility coefficient for electrons, has been determined as a function of E/p, the ratio of the electric field to pressure, in He, Ar, N_2, H_2, D_2, CO, and CO_2. Special interest is centered on the low-temperature, low-E/p data which are essential for the determination of low-energy elastic and inelastic cross sections. The lowest temperature of operation is either 77°K or the boiling point of the gas being measured, whichever is higher. The lowest E/p value is well within the thermal range where $D/\mu=kT/e$. A careful analysis of the operation of the experimental tube is presented along with a method for removing inconsistencies in the results which arise from a conventional interpretation of the data.

I. INTRODUCTION

ONE of the objectives in the field of atomic physics is the determination, as a function of energy, of the elastic and inelastic cross sections of atoms and molecules for electron impact. These can be obtained directly from monoenergetic electron beam experiments for electron energies greater than about 0.1 eV. Due to low-beam intensities and the existence of contact potentials which introduce unknown changes in the beam energy, cross sections cannot be determined from such experiments at lower energies. Instead, swarm experiments using electrons with a distribution of energies, must be resorted to. Such experiments yield the mobility, μ, and the diffusion coefficient, D, as functions of the electric field, E, the gas density, N, and temperature, T. Simple arguments[1] can be used to show that μN, DN, and D/μ must be functions of E/N and T alone. The analysis of these coefficients to obtain the pertinent cross sections as a function of energy is a complicated process, which cannot be accomplished without extensive and accurate data. If swarm experiments are carried out on atomic gases at low enough electron energies, only the elastic cross section is important. Data from a single pertinent experiment, such as a measurement of mobility, are then sufficient for the evaluation[2,3] of a consistent cross section. For a molecular gas at comparable energies, the inelastic cross sections corresponding to rotational and vibrational excitation must also be considered. For the determination of the various cross sections[4–6] in this case, a more extensive theory involving the inelastic processes must be utilized as well as further experimental information, such as that provided by a measurement of D/μ.

Many D/μ measurements exist in the literature,[7–15] all following, more or less, the methods of Townsend. They are all inadequate for the present purposes, to a greater or lesser extent, because of their generally limited accuracy, and their use of electron swarms with energies well above the onset of the rotational and vibrational processes which are of special interest to us. We, therefore, extend the earlier studies of simple molecular gases to much lower energies by working at lower temperatures and lower electric fields. We attempt to obtain greater accuracy by working over much wider extremes of the various experimental parameters. This enables us to employ a method for removing inconsistencies in the D/μ results which arise, when a conventional interpretation of the data is used. As one test of this new method, D/μ measurements are also made in some atomic gases for which D/μ has been predicted[2,3] from mobility measurements.

Even though it is clear that detailed calculations are needed for an accurate determination of cross sections, their gross features are often revealed in D/μ vs E/p curves. This follows from the fact that D/μ is approximately equal to the average electron energy, which is, in turn, sensitive to variations in the different cross sections. At low enough E/p, the electrons are in equilibrium with the gas, and thus $D/\mu=kT/e$. As E/p is increased, the average electron energy and D/μ rise well above this value. In the simple case where only a constant elastic cross section is involved, D/μ increases linearly with E/p for D/μ values above kT/e. If, how-

* This work was supported in part by the Air Force Special Weapons Center and by the Advanced Research Projects Agency through the Office of Naval Research.

[1] A. V. Engel and M. Steenbeck, *Elektrische Gasentladungen* (Verlag Julius Springer, Berlin, 1932), Vol. II, Chap. 1, p. 95.
[2] L. S. Frost and A. V. Phelps (private communication).
[3] L. S. Frost and A. V. Phelps, Bull. Am. Phys. Soc. **5**, 371 (1960).
[4] L. G. H. Huxley, Australian J. Phys. **9**, 44 (1959, and L. G. H. Huxley, J. Atmos. and Terrest. Phys. **16**, 46 (1959).
[5] L. S. Frost and A. V. Phelps, *Proceedings of the Fifth International Conference on Ionization Phenomena in Gases, Munich, 1961* (North-Holland Publishing Company, Amsterdam, 1962), Vol. I, p. 192; and Phys. Rev. **127**, 1621 (1962).
[6] A. G. Engelhardt and A. V. Phelps, Bull. Am. Phys. Soc. **7**, 398 (1962).
[7] J. S. Townsend and V. A. Bailey, Phil. Mag. **46**, 657 (1923).
[8] J. S. Townsend and V. A. Bailey, Phil. Mag. **44**, 1033 (1922).
[9] J. S. Townsend and V. A. Bailey, Phil. Mag. **42**, 873 (1921).
[10] R. W. Crompton and D. J. Sutton, Proc. Roy. Soc. (London) **A215**, 467 (1952).
[11] R. W. Crompton and B. I. H. Hall; data are presented by L. G. H. Huxley, J. Atom. and Terrest. Phys. **16**, 46 (1959).
[12] B. I. H. Hall, Australian J. Phys. **8**, 468 (1955).
[13] M. F. Skinker and J. V. White, Phil. Mag. **46**, 630 (1923).
[14] M. F. Skinker, Phil. Mag. **44**, 994 (1922).
[15] J. B. Rudd; data are presented by R. H. Healey and J. W. Reed, *The Behavior of Slow Electrons in Gases* (Amalgamated Wireless Limited, Sydney, 1941), Chap. 4, p. 98.

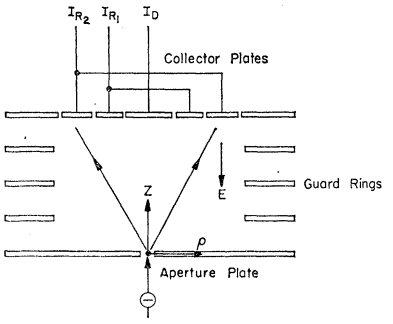

FIG. 1. A schematic diagram of the electrode arrangement for the D/μ tube. The collector plates are in the form of a central disk, D, and two concentric rings, R_1 and R_2. The inner current ratio is I_D/I_{R_1}, while the outer ratio is I_{R_1}/I_{R_2} where I_D, I_{R_1}, and I_{R_2} are the currents to the D, R_1, and R_2, respectively.

ever, the elastic cross section increases or decreases with electron energy, D/μ varies with E/p correspondingly, less or more rapidly than linearly. In a similar fashion, the onset of an inelastic process is sometimes evident on a D/μ curve as a sudden decrease of slope. These general ideas will be used to discuss qualitatively the gross features of our results. Justifications for the above statements and further details can be found in the literature.[5,16]

II. THEORY OF THE EXPERIMENTAL METHOD

Figure 1 shows a schematic diagram of an electrode arrangement of the kind used in the determination of D/μ by the Townsend method. In this type of tube, electrons which have passed through the defining aperture spread by radial diffusion while drifting from the aperture to the collector plate under the influence of the uniform electric field, $\mathbf{E}$. To measure this spread, the collector plate is divided into concentric rings, and the ratio of the currents to any two of these rings is determined. The relationship between these current ratios and D/μ will now be obtained.

The electron current density, $\mathbf{J}$, at any point in the region between the aperture and collector plates is assumed to be given by

$$\mathbf{J}=-D\nabla n-\mu\mathbf{E}n,$$

where D is the diffusion coefficient, μ the mobility, and n the electron density. Departures from this relation due to electron-density gradients are neglected. Their effect is currently being investigated and is believed to be small in our experiments.

For nonattaching gases and when ionization is not significant, $\nabla\cdot\mathbf{J}$ is equal to zero. Therefore, the differential equation governing the density is

$$\nabla\cdot(D\nabla n+\mu\mathbf{E}n)=0. \tag{1}$$

When $\mathbf{E}$ is uniform and pointing in the negative z direction, this reduces to

$$\nabla^2 n-2\beta\partial n/\partial z=0, \tag{2}$$

where $\beta=\mu E/2D$. The solution of Eq. (2) should satisfy the usual boundary conditions, that n equals zero on the collector plate, the walls (guard rings), and on the aperature plate, except within the area of the aperture where the density is finite due to the influx of electrons. However, for the tube geometries and the range of experimental conditions covered in the present study, the effect of the walls and the finite size of the aperture is relatively small. Therefore, the solution for the limiting case of no walls and a point aperture will be considered first, and then the effect of the walls and a finite aperture will be discussed as corrections to this solution.

Huxley[17] has obtained the solution to Eq. (2) for the limiting case of no walls and a point aperture. A derivation based on his approach can be given as follows: The solution of Eq. (2) can be written as $n=e^{\beta z}\varphi$, where φ must then satisfy

$$\nabla^2\varphi-\beta^2\varphi=0. \tag{3}$$

A dipole-like solution that satisfies Eq. (3) is

$$\varphi_D=A(\partial/\partial z)(e^{-\beta r}/r),$$

where r is the distance from the pole. By placing dipoles at $z=0, \pm 2d, \pm 4d$, etc., where d is the distance from the aperture plate to the collector plate and the origin is taken at the aperture, a solution of Eq. (3) is obtained that is zero on the collector plate and zero on the aperture plate except at the aperture itself. This solution can be written in the form

$$\varphi=A\sum_{k=-\infty}^{\infty}(\partial/\partial z)(e^{-\beta r_k}/r_k), \tag{4}$$

where $r_k(\rho,z)=(\rho^2+z_k^2)^{1/2}$ and $z_k=(z-2kd)$.

Now the current density at the collector plate is entirely due to diffusion and is, therefore, given by

$$J=-D(\partial n/\partial z)_{z=d}.$$

Substituting for n, this expression yields[18]

$$J=-DA\left\{\frac{\partial}{\partial z}\left[e^{\beta z}\sum_{k=-\infty}^{\infty}\frac{\partial}{\partial z}\left(\frac{e^{-\beta r_k}}{r_k}\right)\right]\right\}_{z=d}.$$

Performing the differentiation outside the summation sign and recognizing that $n=0$ at $z=d$, it follows that

$$J=-DAe^{\beta d}\left[\sum_{k=-\infty}^{\infty}\frac{\partial^2}{\partial z^2}\left(\frac{e^{-\beta r_k}}{r_k}\right)\right]_{z=d}.$$

[16] L. B. Loeb, *Basic Processes in Gaseous Electronics* (University of California Press, Berkeley, 1955), Chap. 4.

[17] L. G. H. Huxley, Phil. Mag. **30**, 396 (1940).

[18] It is at this point in the derivation that an error was made by Huxley which invalidated his final relation between D/μ and the current ratio. While in a subsequent note (reference 20) this error was acknowledged, the complete expression for the collector currents has not appeared in the literature.

TABLE I. Electrode dimensions of the D/μ tubes.

	Short tube (in.)	Long tube (in.)
Drift distance (d)	0.5	3.5
Disk radius	0.242	0.242
First ring outer radius	0.477	0.477
Second ring outer radius	0.704	0.704
Aperture radius (a)	0.05	0.05
Guard ring inner radius (b)	1.5	1.5
Guard ring spacing	0.125	0.5

Now the total current, I, to one of the individual collectors is given by

$$I=2\pi\int_{\rho_1}^{\rho_2}J\rho d\rho=-2\pi DAe^{\beta d}\int_{\rho_1}^{\rho_2}\left[\sum_{k=-\infty}^{\infty}\frac{\partial^2}{\partial z^2}\left(\frac{e^{-\beta r_k}}{r_k}\right)\right]_{z=d}\rho d\rho,$$

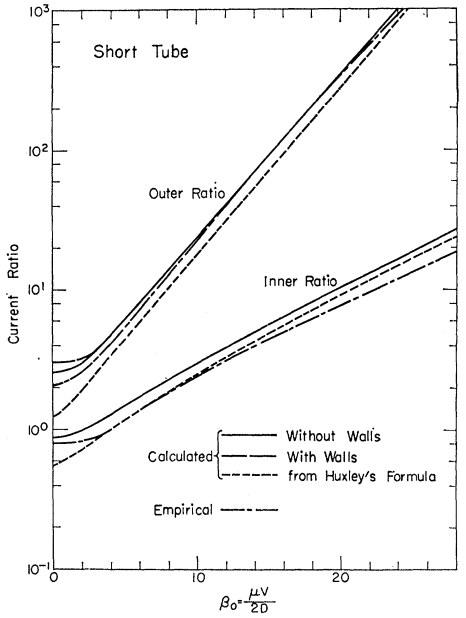

FIG. 2. Inner and outer current ratio vs β_0 curves for the short tube. The curves represent both the calculated and empirical relations discussed in the text.

where ρ_1 and ρ_2 are the inner and outer radius of this collector. By interchanging the order of integration and differentiation and changing the variable of integration to r_k, the integration can be carried out to give

$$I=\frac{2\pi DAe^{\beta d}}{\beta}\sum_{k=-\infty}^{+\infty}\left[\frac{\partial^2}{\partial z^2}(e^{-\beta r_k})\right]_{r_k(\rho_1,d)}^{r_k(\rho_2,d)}.$$

After carrying out the differentiation, and noting that the dipoles for $k=0$ and $+1$ each contribute the same amount to the above sum, as do the pair of dipoles with

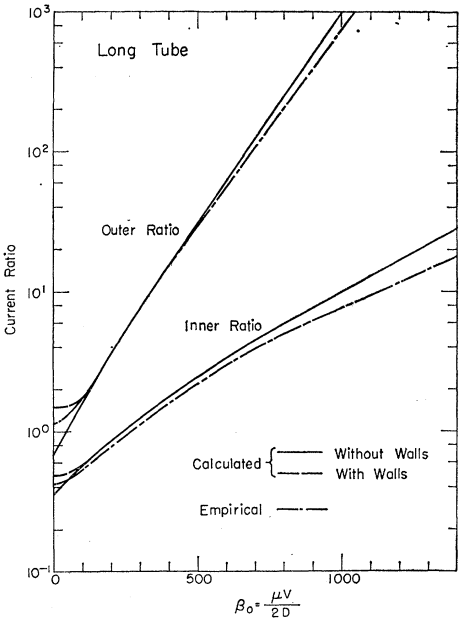

FIG. 3. Inner and outer current ratio vs β_0 curves for the long tube. The curves represent both the calculated and empirical relations discussed in the text.

$k=-1$ and $+2$, etc., the sum can be written

$$I=4\pi DAe^{\beta d}\sum_{k=0}^{\infty}\left[\frac{e^{-\beta r_k}}{r_k^3}(\beta r_k z_k^2-\rho^2)\right]_{r_k(\rho_1,d)}^{r_k(\rho_2,d)}. \quad (5)$$

The dependence of the current ratios on β can now be obtained using this expression.

In the present study two different tube geometries were used and the pertinent dimensions for these geometries are given in Table I. The design of the collector plate, which is in each case composed of two concentric rings and a central disk, allows the determination of two independent current ratios, the "inner" ratio of the disk current to the first ring current and the "outer" ratio of the first ring current to the outer ring current. The calculated dependence of the two current ratios on the dimensionless quantity $\beta_0=\beta d=\mu V/2D$ is given in Figs. 2 and 3 for the case discussed above of no walls and a point aperture. It should be remarked that when $\beta_0\geq 3$ for the short tube and for all β_0 for the long tube, the first term in the summation of Eq. (5) gives the current ratio to within 1% of the exact value.

Townsend has given a different solution[19] to Eq. (2) that takes the walls into account, assumes a uniform electron density across a finite aperture, and ignores the effect of the collector plate. We have extended Townsend's solution to include the collector plate boundary condition. This solution is given by

$$n(\rho,z)\propto e^{\beta z}\sum_{j=1}^{\infty}\frac{J_1(k_ja/b)J_0(k_j\rho/b)\sinh\{[\beta^2+(k_j/b)^2]^{1/2}(d-z)\}}{k_jJ_1^2(k_j)\sinh\{[\beta^2+(k_j/b)^2]^{1/2}d\}}.$$

[19] J. S. Townsend, *Electricity in Gases* (Oxford University Press, London, 1915), Chap. 5.

Then the total current to any one of the collectors is given by

$$I \propto \sum_{j=1}^{\infty} \frac{J_1(k_j a/b)[\beta^2+(k_j/b)^2]^{1/2}[\rho_2 J_1(k_j\rho_2/b)-\rho_1 J_1(k_j\rho_1/b)]}{k_j^2 J_1^2(k_j)\sinh\{[\beta^2+(k_j/b)^2]^{1/2}d\}},$$

where J_0 and J_1 are Bessel functions of the first kind, k_j is the jth root of J_0, a is the aperture radius, d the drift distance, and b the wall radius. In these expressions, all factors not affecting the current ratios have been dropped. The current ratios calculated from this solution are shown in Figs. 2 and 3. Comparing these ratios with those from the dipole solution, it is to be noted that the effect of the walls becomes smaller as β_0 is increased. For the inner ratio of the short tube, the effect of the walls is negligible for all β_0 and, therefore, the corresponding curve is indistinguishable from the "without walls" curve of Fig. 2 and is not shown. It should be remarked that, since the actual walls are in the form of guard rings and not the perfect cylindrical boundary assumed in obtaining the above solution, the calculated wall effect is not directly applicable to our tube but only gives a qualitative indication of the value of β_0 below which the walls become important.

While the Townsend-type solution does take the size of the aperature into account, it cannot be easily evaluated at large β_0, where the effect of the aperture size is most noticeable, because of its slow convergence. Therefore, we have used the dipole solution given by Eq. (4) as a basis for building up a solution valid for the case of a finite aperture and large β_0. This was accomplished by taking that summation of point dipole solutions which corresponds to covering the aperture area with a uniform distribution of dipoles. In this way, a solution of Eq. (3) is obtained which meets the boundary conditions at the collector and aperture plates and gives a uniform electron density over the aperture area. The resulting expression for the current to any one collector (which is good to first order in the ratio of aperture to disk radius) is given by

$$I \propto \sum_{k=0}^{\infty}\left[\frac{2}{\beta\rho a}\frac{e^{-\beta r_k}}{r_k^3}\left\{I_1\left(\frac{\beta\rho a}{r_k}\right)\left[2r_k^2-\beta(3z_k^2r_k+r_k^3)+\beta^2\left(z_k^2r_k^2+\frac{z_k^2\rho^2a^2}{r_k^2}\right)\right]+I_0\left(\frac{\beta\rho a}{r_k}\right)[2\beta^2z_k^2\rho a-\beta\rho r_k a]\right\}\right]_{r_k(\rho_1,d)}^{r_k(\rho_2,d)},$$

where I_0 and I_1 are Bessel functions of the imaginary type. It can be easily shown that this expression reduces to Eq. (5) in the limit of zero aperture size. The effect of the finite aperture size used in our tubes was determined from the above expression. It causes a shift of the current ratio curves to higher β_0 by an amount that is less than 5% for both the short and long tubes for the entire β_0 range covered in the present study. If a more reasonable assumption had been made about the electron density across the aperture, for example, a parabolic distribution with the density equal to zero on the aperture boundary, an even smaller shift of the curves would result. Because of the small, as well as uncertain, size of this correction, the current ratio curves obtained for the finite aperture are not shown in Figs. 2 and 3.

A current ratio versus β_0 relationship that has been used in many of the more recent measurements[10–12] of D/μ was originally proposed by Huxley.[17] The ratio curves calculated from this "Huxley formula" differ appreciably from the other calculated curves for the short tube as is made evident in Fig. 2. For the long tube, however, the "Huxley formula" gives essentially the same ratio curve as that obtained for the case of no walls and a point aperture which was discussed above. While the use of this formula was ultimately justified by Huxley and Crompton[20] on only an empirical basis, it does result from the solution of Eq. (2) for the case of electrons issuing from a point aperture in an infinite plane when the effect of the collector plate boundary condition is ignored and the currents which are used to calculate the ratios include only the contribution due to mobility. In essence this solution is very similar to that used by Townsend except Townsend did take the walls and the finite aperture into account.

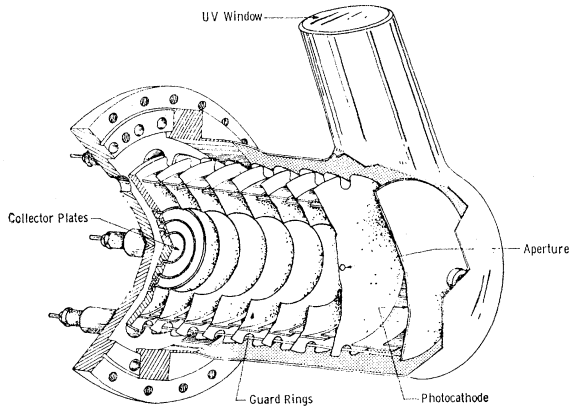

FIG. 4. Cutaway view of the electrode structure and vacuum envelope of the long tube.

III. EXPERIMENTAL APPARATUS AND PROCEDURE

Figure 4 shows a cutaway view of the long experimental tube. The envelope is constructed of Pyrex, Kovar, and nonmagnetic stainless steel. The various electrodes are fabricated from 0.015-in. advance sheet

[20] L. G. H. Huxley and R. W. Crompton, Proc. Phys. Soc. (London) **B68**, 381 (1955).

except for the collector structure which is machined from heavier stock. The 0.005-in. spacing of the overlapping collector electrodes minimizes the penetration of unknown fields into the drift region. A series of guard rings with attached shields establishes a drift region with an approximately uniform field.

A typical ultrahigh vacuum system[21] is used, with a vacuum of 10^{-9} Torr (1 Torr≡1 mm Hg) readily obtainable. The gases investigated are of Airco research grade except for the case of D_2 which is of poorer quality. A mass spectroscopic analysis of the D_2 shows the presence of 2% HD, traces of other gases, and water. The water was removed with a liquid nitrogen trap. The gas pressure is measured with an accuracy of better than 1% with a diaphragm manometer.[22] For measurements at low temperatures, the experimental tube is immersed in a bath of liquid nitrogen, liquid argon, or a carbon dioxide-methanol slush. Electrical connections to the various terminals are made of fine, high-resistance wire to reduce the heat flow through these wires from room temperature.

Ultraviolet light enters the tube through a fused silica window and ejects electrons from an evaporated or electroplated gold cathode. These electrons are drawn to the aperture plate by a field equal to that in the drift space. Light scattered through the aperture is minimized by polishing the photocathode and by blackening all other surfaces in this region. It has been found that if all the electrodes in the tube except the cathode are coated with colloidal graphite, one obtains surfaces with a low reflectivity and low contact potentials.[23]

A 100-W mercury lamp, which is the source of ultraviolet light, is made a part of a negative feedback loop, designed to keep the cathode current constant to within 0.1%. When the experimental tube is evacuated, this current is about 2×10^{-7} A; when it contains a gas, the current ranges from 10^{-8} to 10^{-10} A. Approximately 0.1% of this current passes through the aperture. A switch grounds two of the collector electrodes while connecting the third to a vibrating reed electrometer with an effective noise current of about 10^{-16} A and a time constant of 10 sec. The tube currents are sufficiently small so that no effect due to space charge is observed. Another effect that is not always negligible, however, is that due to electron emission from various surfaces in the tube by ultraviolet light scattered through the aperture. To measure these currents, the cathode is made sufficiently positive with respect to the aperture, so that no electrons from the cathode can reach the aperture, and then only the currents due to scattered light will reach the collectors. These currents, which are at most 5% of the total currents, are subtracted from them to give the desired currents. The ratio of the collector currents, as well as the electrode potentials, can be measured with an accuracy of about 1%. The accuracy of β_0, which is read from the graphs of current ratio vs β_0, differs from the accuracy of the measured ratio by a factor which depends upon the slope of these curves. When β_0 is less than a critical value (which is about 75 for the long tube and 3 for the short tube) this factor is greater than 5, making the errors in β_0 intolerable.

It is desirable to make collector current measurements over as wide a range of fields and pressures and to as low a temperature as possible. The absolute low-temperature limit is approximately the boiling point of the gas involved. However, for practical reasons no measurements are taken below liquid nitrogen temperatures. The upper pressure limit is set at one atmosphere by the tube construction; the lower pressure limit is that pressure at which β_0 is less than the critical β_0, mentioned above, for all attainable fields. The upper limit to the field used is set by either the breakdown strength of the gas involved, or a β_0 value so high that the currents to the outer collector rings are too small to be measured. The low field limit is set by one of the following: collector currents which are too small to be measured, a β_0 value less than the critical value discussed above, or the effect of contact potentials. The contact potentials in our tubes are estimated[23] to be about 10 mV. The fields are, therefore, approximately uniform only when the voltages between the various electrodes are much greater than 10 mV. When this condition is not satisfied, i.e., when the voltage applied between the aperture and collector plates is less than about 1 V, irregular results are observed. For most gases, the pressure range investigated covers a factor of about 100, and at each pressure the field is varied by a factor of about 100.

IV. TEST OF THE THEORY WITH HELIUM

Extensive measurements were first made with helium in the long tube at 300 and 77°K. Helium was used because it is an especially simple gas and because its D/μ values have been predicted by Frost and Phelps[2] from the mobility data of Phelps, Pack, and Frost.[24] Figure 5 shows the predicted curves of D/μ vs E/p_{300} for helium at 300 and 77°K. Here p_{300} is a normalized gas pressure given by $p_{300}=300p_T/T$, where T and p_T are the temperature and pressure at which a measurement is made. The ratio of the gas density, N, to p_{300} is 3.22×10^{16} cm^{-3} Torr^{-1}. Also shown in Fig. 5 are the experimental points obtained from the measured current ratios and the current ratio vs β_0 curves shown in Fig. 3 which were calculated assuming the use of a point aperture without walls. The range of E/p_{300} covered at

[21] D. Alpert, in *Handbuch der Physik*, edited by S. Flügge (Springer-Verlag, Berlin, 1958), Vol. XII, p. 609.
[22] D. Alpert, C. G. Matland, and A. O. McCoubrey, Rev. Sci. Instr. **22**, 370 (1951).
[23] J. H. Parker, Jr. and R. W. Warren, Rev. Sci. Instr. (to be published).
[24] A. V. Phelps, J. L. Pack, and L. S. Frost, Phys. Rev. **117**, 470 (1960); J. L. Pack and A. V. Phelps, *ibid.* **121**, 798 (1961).

each pressure and temperature is indicated on the graph by the length of a horizontal line labeled with the appropriate value of p_{300}. The assumption that no walls are present is unimportant, since the experimental points always correspond to β_0 values such that the "with walls" and the "without walls" curves of Fig. 3 have merged. The assumption that a point aperture is used is relatively unimportant since, as mentioned previously, the effect of the finite aperture size is to shift the curve of Fig. 3 to the right by a few percent which causes the experimental points of Fig. 5 to be shifted down by a few percent. The use of the "Huxley" curve of Fig. 3 leads to results insignificantly different from those found with the more correct curve. The agreement shown in Fig. 5, however, is not good; the approximately 30% spread of the experimental points is much more than would be expected from experimental sources. It is not a random spread, but could be greatly reduced if a slightly different ratio vs β_0 curve could be chosen due to the inclusion in the theory of some previously ignored factor. Such a modification of the theory will now be discussed.

If the idealized geometry of the experimental tube is distorted by a translation of the collector structure, the electric field will still be uniform and Eq. (2) will still determine the electron density. The current ratios, however, will now be new functions of β_0. For a more general distortion, $\mathbf{E}$ will be nonuniform and can be written $\mathbf{E}=(V/d)\mathbf{F}$, where $\mathbf{F}$ is a function only of position. If D and μ are constants, which will now be strictly true only in the thermal region, Eq. (1) becomes $\nabla^2 n-(2\beta_0/d)\nabla\cdot n\mathbf{F}=0$. The current ratios derived from this equation can still be expressed solely in terms of β_0. Only when the variation of D and μ with position is taken into account does one find the current ratios to depend, and then fairly weakly, upon factors other than β_0. Thus, depending upon what kinds of distortion are most important in our tube, a choice of the right current ratio vs β_0 curve can either exactly or, at worst, approximately compensate for the distortions.

As a sensitive test of the presence of some kinds of geometric errors, the collector rings were rebuilt with the disk and first ring split in half along a diameter. The currents received by the two identical halves differ, typically, by 10%. Certainly, then, even though the tube construction was very accurately done, some distortion is present. If this distortion were simply a sidewise translation of the collector structure sufficient to explain the current asymmetry, then its effect on the current ratios would be too small to explain the observed deviations in D/μ. However, more complicated distortions, for which estimates have not been made due to their difficulty, could cause the observed deviations. Factors other than geometric that have been investigated and found to be too small to seriously affect the current ratios, are those due to contact potentials, space charge, insulating surface layers, magnetic fields, and incorrect temperature measurements.

On the assumption that all the systematic deviation shown in Fig. 5 are due to geometric errors, there should be an empirical ratio vs β_0 curve which removes the observed deviations. If such a unique curve exists, it can be found by the graphical process described in the appendix using only the assumptions: 1) that each of the current ratios is a function of β_0 alone, 2) that D/μ is a function of E/p_{300} alone, and 3) that the Einstein relation holds, i.e., the limiting value of D/μ at low E/p is kT/e. In Fig. 3 is shown the empirical ratio vs β_0 curves developed independently for the inner and outer ratios of the long tube from the data for helium at 300°K. Figure 6 shows D/μ vs E/p_{300} for helium at 300 and 77°K, calculated anew from these empirical curves. The consistency that can be achieved by this technique is shown by the following: (1) the empirical current ratio vs β_0 curves can be precisely and uniquely determined, reducing the spread in the D/μ plot at 300°K

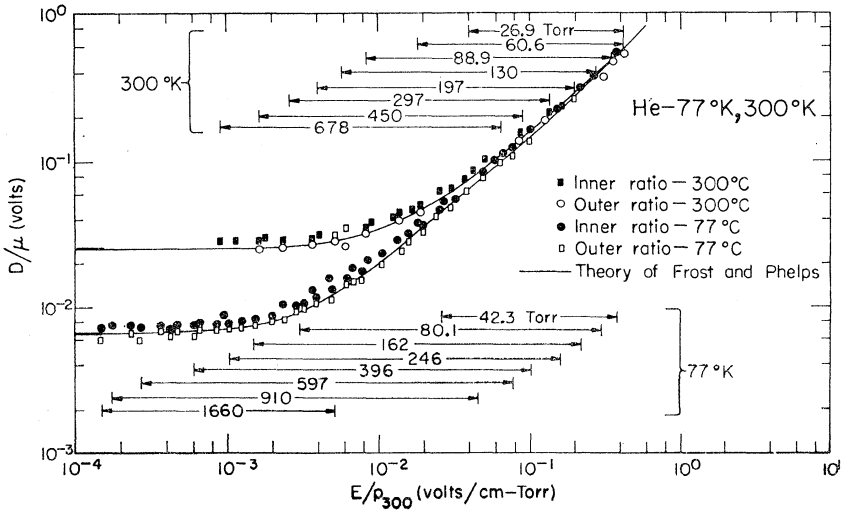

FIG. 5. D/μ vs E/p_{300} for helium at 77 and 300°K. The results were obtained from the measured inner and outer current ratios of the long tube and the calculated current ratios vs β_0 curves of Fig. 3 for the case of no walls and a point aperture. The range of E/p_{300} covered at a given pressure and temperature is indicated by the horizontal line labeled with the corresponding value of T and p_{300}. p_{300} is a normalized gas pressure given by $p_{300}=300p_T/T$, where T and p_T are the temperature and pressure at which a measurement was made. The pressure unit used is the Torr, where 1 Torr≡1 mm Hg. The values of kT/e corresponding to the temperatures at which the measurements of the present and earlier investigators were taken are indicated by bold lines at the left margin of the graphs.

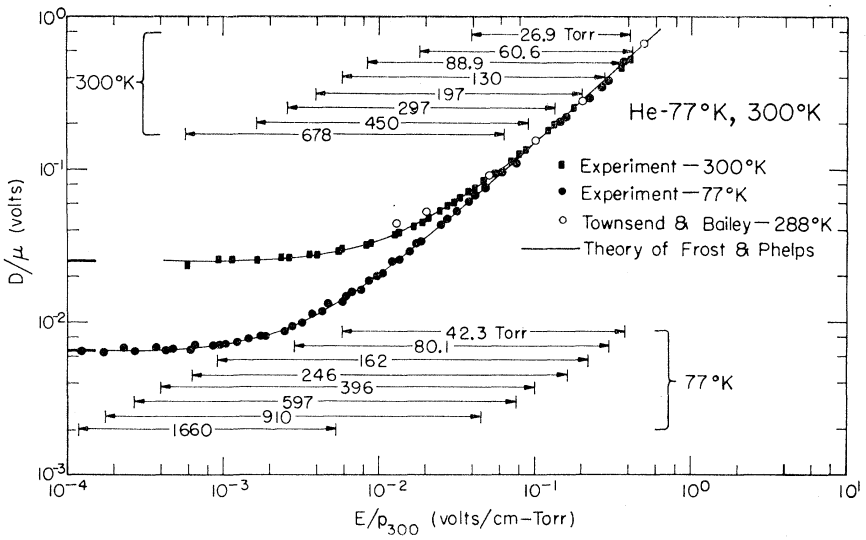

FIG. 6. D/μ vs E/p_{300} for helium at 77 and 300°K. The results were obtained from the empirical current ratio curves of Fig. 3 and the same data used for Fig. 5. Each point shown corresponds to the average of the D/μ values obtained from the inner and outer ratio.

by a factor of 5; (2) the values of D/μ calculated from the inner and outer ratios agree with each other and the predicted curve within a few percent; (3) the agreement between D/μ calculated from the two ratios and the predicted curve is equally good at 77°K; (4) the above statements are equally true of the short tube for which the empirical curve is shown in Fig. 2; (5) D/μ determined with the short and long tube agree with each other; and finally, (6) as will be shown, the results found for every other gas studied by using the empirical ratio vs β_0 curve which was derived from the helium data at 300°K, have the correct low-E/p limit, give good agreement between the inner and outer ratios, and have very little spread. The remaining spread in the data of a few percent is random and what one would expect from an accumulation of errors from the voltage, pressure, and current measurements. In addition to correcting for various geometric errors, this empirical approach takes into account the true wall effect, and thus the empirical ratio vs β_0 curve can be used at low β_0 values where the walls are important.

V. DISCUSSION OF RESULTS

The results[25] discussed below and shown in Figs. 6–12 are all derived from measurements with the long tube and the empirical ratio vs β_0 curves obtained for helium at 300°K. The results obtained from the inner and outer ratio show no systematic difference and so only the average is shown on the graphs. These results are consistent with less extensive but similar measurements carried out with the short tube. The range of E/p_{300} covered at each pressure and temperature studies is indicated on the graphs. The values of kT/e corresponding to the temperatures at which the measurements of the present and earlier investigations were taken are indicated by bold lines at the left margin of the graphs.

Helium

The results for helium at 300 and 77°K shown in Fig. 6 agree within the experimental error of a few percent with that predicted by Frost and Phelps[2] and shown on the graph as a solid curve. The agreement with the results of Townsend and Bailey[7] are good at high D/μ, while at lower D/μ values their results appear to be high. A possible explanation for this deviation is the same as for our initial spread, i.e., that almost any geometric distortion of the experimental tube affects the current flow so as to give a larger apparent D/μ, an

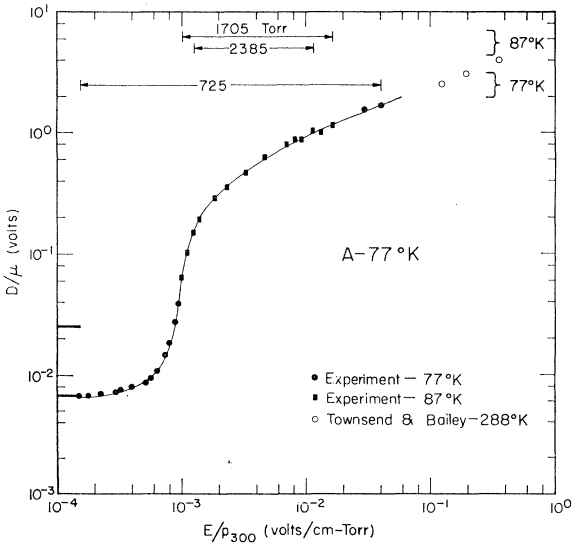

FIG. 7. D/μ vs E/p_{300} for argon at 77°K. The empirical current ratio curves were used, and the average D/μ values obtained from the inner and outer ratio are shown. The solid curve is the best fit to these values.

[25] These results are available in tabular form in the Westinghouse Research Laboratories Scientific Paper 62-908-113-P6 (unpublished).

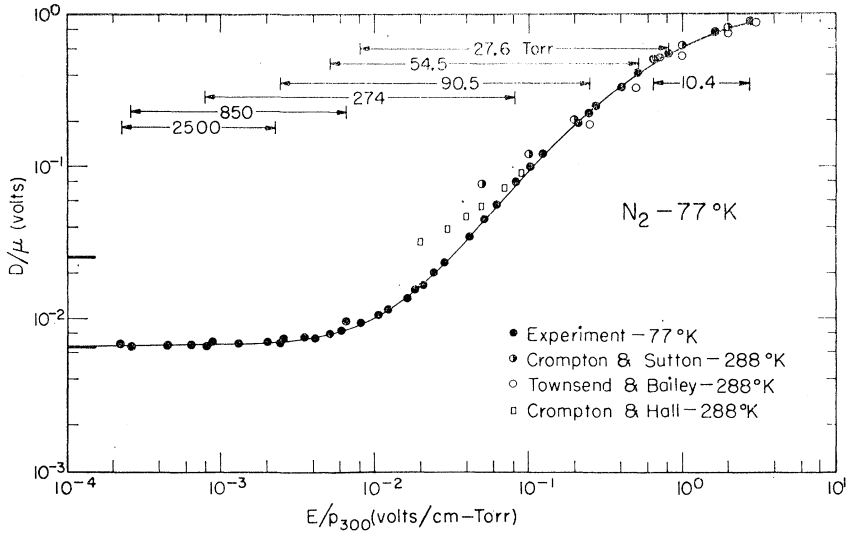

FIG. 8. D/μ vs E/p_{300} for nitrogen at 77°K. The empirical current ratio curves were used, and the average D/μ values obtained from the inner and outer ratio are shown. The solid curve is the best fit to these values.

effect especially noticeable at low D/μ values. The shape of the D/μ vs E/p_{300} curve at high E/p_{300}, i.e., its constant slope of about 45°, is due to an almost constant elastic cross section for He as a function of energy.

Argon

Figure 7 shows the present data for argon at 77°K and 87°K and that of Townsend and Bailey[9] at 288°K. Due to the low E/p_{300} values that must be covered in argon, unusually high gas densities are essential. The highest possible density is achieved in our tubes at atmospheric pressure and 87°K, the boiling point of argon. The maximum pressure and, therefore, density attainable at 77°K is so low that trustworthy data can be obtained only over a part of the E/p_{300} range of interest. The rest of the E/p_{300} range is covered by the 87°K data. When D/μ is sufficiently high compared to kT/e, it is almost independent of the gas temperature and, therefore, the high D/μ values calculated from the 87°K data are assumed[26] to be equally representative of argon at 77°K. The solid curve shown in Fig. 7 is the best fit to the combined data and, therefore, this curve is taken to represent D/μ vs E/p_{300} at 77°K. The data of Townsend and Bailey shown in Fig. 7 are taken at E/p_{300} values so high that they do not overlap the present results but are found to be a smooth continuation of them.

In principle, it should be possible to predict D/μ for argon from mobility measurements in the same way as was done for helium. However, because of the large variations of the elastic cross section with electron energy, the calculation is more difficult than for helium.

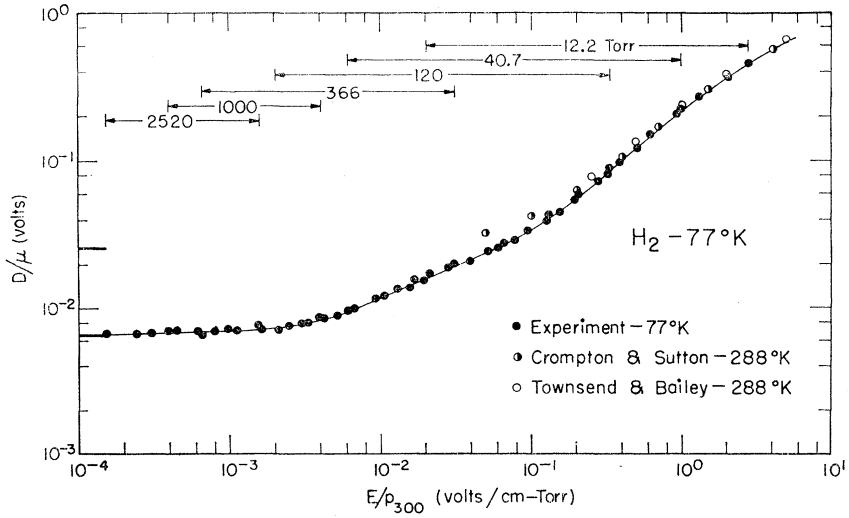

FIG. 9. D/μ vs E/p_{300} for hydrogen at 77°K. The empirical current ratio curves were used, and the average D/μ values obtained from the inner and outer ratio are shown. The solid curve is the best fit to these values.

[26] Estimates have been made by L. S. Frost and A. V. Phelps (private communication) of the dependence of D/μ on temperature in the E/p range within which the 87°K data were taken. These estimates indicate that 77°K values would lie within the experimental spread of the measured 87°K values.

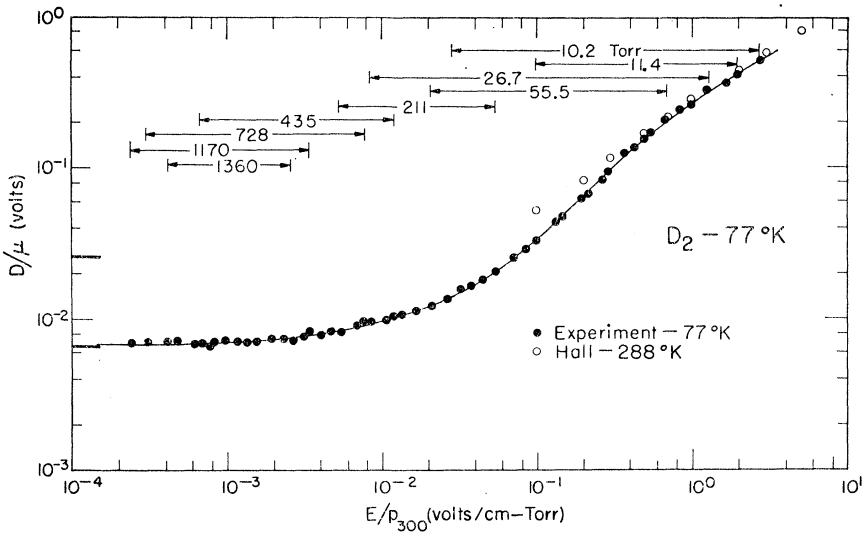

FIG. 10. D/μ vs E/p_{300} for deuterium at 77°K. The empirical current ratio curves were used, and the average D/μ values obtained from the inner and outer ratio are shown. The solid curve is the best fit to these values.

Preliminary results by Frost and Phelps[3] agree with the combined data of Fig. 7 within 20%. The rapid rise and subsequent flattening of the D/μ vs E/p_{300} curve at high E/p_{300} is due to the marked minimum in the elastic cross section of argon as a function of energy.

Nitrogen

D/μ cannot be predicted from mobility measurements alone for any of the molecular gases. A comparison it shown in Fig. 8 between the present measurements as 77°K and those of Townsend and Bailey,[9] Crompton and Sutton,[10] and Crompton and Hall,[11] all at 288°K. Part of the disagreement with the earlier data at low D/μ is due to the difference in the temperatures at which the measurements were taken. The smooth curve shown for this gas and those that follow is the best fit of the data. While there is no obvious structure in the D/μ curves which can be related to the onset of inelastic processes for this and the two following gases, H_2 and D_2, still a careful analysis[5,6] shows that energy losses due to both rotational and vibrational processes are important in the range of D/μ shown.

Hydrogen

The measurements of Townsend and Bailey,[9] and Crompton and Sutton[10] at 288°K along with those of the present authors at 77°K are shown in Fig. 9. The agreement is good at high D/μ where D/μ is insensitive to temperature.

Deuterium

Figure 10 shows the present data at 77°K and that of Hall[12] at 288°K. Again, the agreement is good at high D/μ.

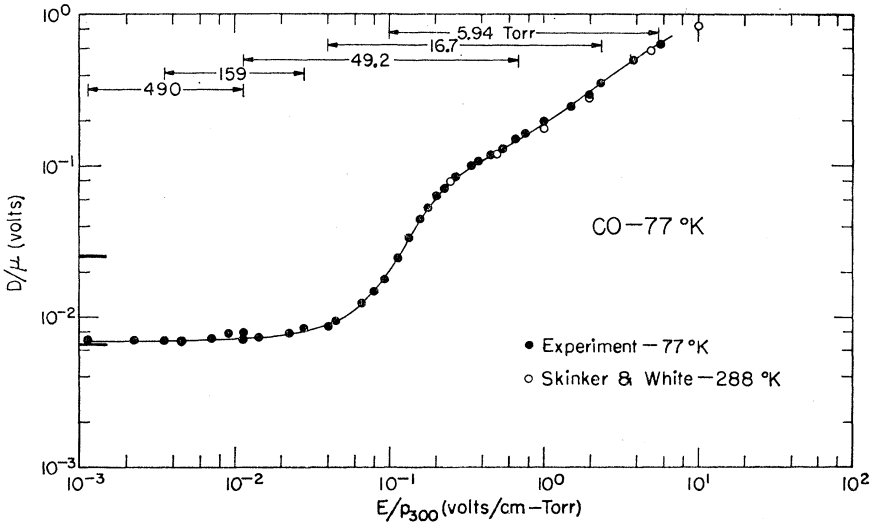

FIG. 11. D/μ vs E/p_{300} for carbon monoxide at 77°K. The empirical current ratio curves were used, and the average D/μ values obtained from the inner and outer ratio are shown. The solid curve is the best fit to these values.

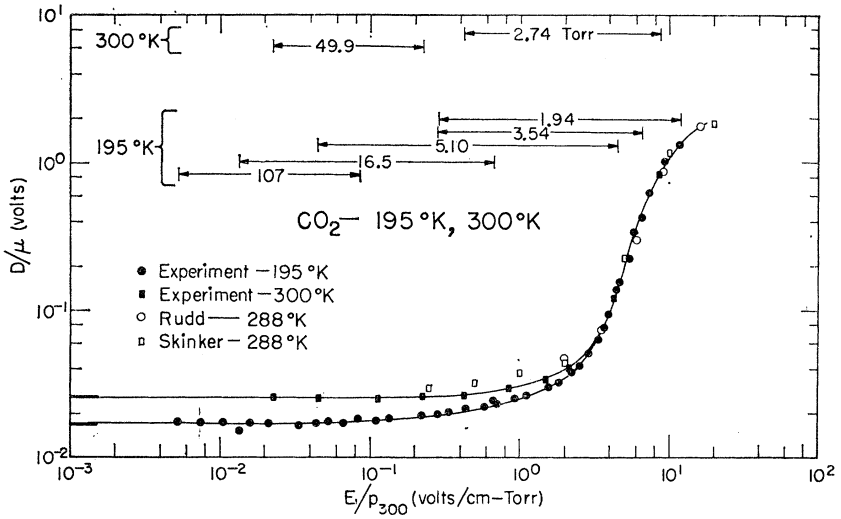

FIG. 12. D/μ vs E/p_{300} for carbon dioxide at 195 and 300°K. The empirical current ratio curves were used, and the average D/μ values obtained from the inner and outer ratio are shown. The solid curve is the best fit to these values.

Carbon Monoxide

Figure 11 shows the good agreement between the present results at 77°K and that of Skinker and White[13] at 288°K. The sudden break in the curve at a D/μ value of about 0.1 V is probably due to the onset of the vibrational excitation process whose energy, determined spectroscopically,[27] is 0.26 eV.

Carbon Dioxide

Since the D/μ curve, as shown in Fig. 12, does not rise from the thermal value until quite high E/p_{300} values are reached, the data taken by Skinker[14] and by Rudd[15] at 288°K come much closer to the thermal region than do other early data for other gases. We, therefore, have made D/μ measurements, not only at 195°K (the boiling point of CO_2), but also at 300°K, in order to compare our results with these earlier ones. The high D/μ values agree quite well, but their low D/μ values are definitely too high, in this case by about 20%. This type of disagreement is similar to that which was found in the comparison of our data with that of Townsend and Bailey for He at 300°K. The rapid rise in D/μ at very high E/p values is related to the strong energy dependence of the relatively large inelastic losses.

VI. SUMMARY

Determinations of D/μ vs E/p_{300} have been made in a variety of atomic and molecular gases down to the thermal limit of $D/\mu=kT/e$ and, in most cases, at the lowest possible temperature. A technique has been developed for determining empirical current ratio vs β_0 curves. These curves differ significantly from the theoretical curves due to, we believe, distortions in the geometry of the experimental tube. These measurements of D/μ will facilitate the determination of the various elastic and inelastic cross sections of the gases investigated at low electron energies.

ACKNOWLEDGMENT

The authors wish to express their appreciation for valuable discussions of this work with the members of the Atomic Physics Group, especially L. S. Frost and A. V. Phelps.

APPENDIX

Graphical Determination of the Empirical Current Ratio vs β_0 Curves

This empirical process is based on the following assumptions: That $\beta_0=\mu V/2D=f(R)$; that $D/\mu=g(E/p_{300})$; and that in the limit of low E/p, $D/\mu=kT/e$. R is any of the current ratios and the functions f and g are to be found. We first note that $\log(V/2)=\log g(E/p_{300})+\log f(R)$ and then start by plotting all the experimental data for helium at 300°K on a graph of R vs V. Smooth curves are now passed through the data points corresponding to each pressure, and a large number of horizontal lines are drawn across the graph at different values of R. A new graph is drawn of $\log(V/2)$ vs $\log(E/p_{300})$ and on it are placed points corresponding to all of the intersections of the horizontal lines and the smooth curves of the first graph. The points corresponding to a given ratio are connected by a smooth curve and labeled by this ratio. This graph is just what is needed, a plot of $\log(V/2)=\log g(E/p_{300})+\log f(R)$, where the dependence of $V/2$ on E/p_{300} and R can be easily separated. To accomplish this separation, the individual curves corresponding to different R values are slid parallel to the $\log(V/2)$ axis until they are all superimposed and, in addition, until

[27] G. Herzberg, *Spectra of Diatomic Molecules* (D. Van Nostrand Company, Inc., Princeton, New Jersey, 1950), Appendix.

$V/2$ at low E/p_{300} values is equal to $kT/e=0.0258$ eV. Then the amount that each curve was shifted equals $\log f(R)$, and the final composite curve is a plot of $\log(D/\mu)$ vs $\log(E/p_{300})$. How well the curves can be superimposed is a good test of the assumptions that have been made. Figures 2 and 3 show the two empirical ratio vs β_0 curves developed in this way for each tube from the data for helium at 300°K.

PHYSICAL REVIEW VOLUME 128, NUMBER 6 DECEMBER 15, 1962

L-Shell Fluorescence Yields of Pt, Tl, and Pb†

R. C. JOPSON, HANS MARK, AND C. D. SWIFT
Lawrence Radiation Laboratory, University of California, Livermore, California
(Received July 23, 1962; revised manuscript received September 10, 1962)

Partial L-shell fluorescence yields for three heavy elements have been measured using an x-ray coincidence counting method. Vacancies in the K shell of the atom are produced either by K-electron capture or internal conversion of a nuclear gamma ray in the K shell. The coincidence rate between the K and L x rays observed after the creation of the K vacancy determines the partial fluorescence yield, ω_{KL}. This quantity is defined as the fluorescence yield of those vacancies in the L shell created by K_{α_1} and K_{α_2} x-ray emission. In some cases, it was also possible to determine the partial fluorescence yield, ω_{LL} of the L shell following L-electron capture. The results obtained are in reasonable agreement with previous measurements. The relationship between ω_{KL}, ω_{LL}, and the fluorescence yields of individual L subshells is discussed.

I. INTRODUCTION

AN atom with a vacancy in one of its inner shells may emit either an x ray or an Auger electron[1,2] which results from the transition of an electron in a higher shell to the vacancy. The fluorescence yield of the shell or subshell is defined as the ratio of the number of characteristic x rays emitted in transitions to this shell or subshell to the number of vacancies created in the shell or subshell

$$\omega=N_x/N_v. \tag{1}$$

There are a number of methods which have been employed to measure ω. The most direct way of determining ω for a given shell is to place a sample in an x-ray beam with a quantum energy sufficiently high to ionize the shell in question. The intensity of the fluorescence x rays emitted by the sample is then compared to the attenuation of the incident beam by the sample. The ratio of these quantities is proportional to the fluorescence yield. Lay[3] has made systematic measurements of a large number of K- and L-shell fluorescence yields using photographic films to make the intensity measurements. Stephenson[4] and Küstner and Arends[5] employed a variation of Lay's method by using ionization chambers rather than photographic plates to determine the beam intensities. Kinsey[6] has computed a number of L-shell yields by comparing the widths of the x-ray absorption edges with those of the emission lines. The width of the absorption line is proportional to the total width of the level and the width of the emission line depends only on the radiative part of the matrix element. The ratio of the two widths is therefore proportional to the fluorescence yield. A large number of other experiments have also been performed, using a radioactive decay process (either electron capture or internal conversion) to create the vacancies in the atomic shells. Since this is the method employed in the present work, appropriate references will be made when individual cases are discussed.

II. EXPERIMENTAL METHODS

In the present experiments, a coincidence counting method previously used by Schmied and Fink[7] and Jopson *et al.*[8] is employed. A vacancy is created in the K shell of the atom either by K capture or internal conversion. About 80% of these vacancies are filled by the emission of K_α x rays in which electrons from the L_{II} and L_{III} subshells make transitions to the K shell. Vacancies in the L_{II} and L_{III} subshells are therefore created and these, in turn, give rise to L x rays or L Auger electrons. The coincidence rate between L and K x rays is given by

$$N_C=N_K a(E_L A_L \Omega_L)\omega_{KL}, \tag{2}$$

where N_K is the number of K x rays observed in the K counter, a is the fraction of these corresponding to K_α transitions, $(E_L A_L \Omega_L)$ is the factor defining the effi-

† Work supported by the U. S. Atomic Energy Commission.
[1] P. Auger, Ann. Phys. (New York) **6**, 183 (1926).
[2] E. H. S. Burhop, *The Auger Effect* (Cambridge University Press, New York, 1952).
[3] H. Lay, Z. Physik **91**, 533 (1934).
[4] R. J. Stephenson, Phys. Rev. **51**, 637 (1937).
[5] H. Küstner and E. Arends, Ann. Physik **22**, 443 (1935).
[6] B. B. Kinsey, Can. J. Research **A26**, 404 (1948).
[7] H. Schmied and R. Fink, Phys. Rev. **107**, 1062 (1957).
[8] R. C. Jopson, H. Mark, C. D. Swift, and J. H. Zenger, Phys. Rev. **124**, 157 (1961).